Analysis of Commonly Used Riprap Design Guides Based on Extended Shields Diagram

HSIEH WEN SHEN and SANG-YI WANG

ABSTRACT

River and coastal engineers are often faced with the task of selecting the appropriate riprap size for bank protection. Several empirical formulae based on field and laboratory tests have been suggested for selecting the maximum size and gradation size distribution of the riprap. To facilitate riprap size selection, several commonly used riprap design guides presented by the U.S. Army Corps of Engineers (for shore protection), the U.S. Bureau of Reclamation (for bank protection), and the California Department of Transportation (for both shore and bank protection) as well as guides from projects sponsored by the FHWA (for energy dissipators related to both culverts and channels) are analyzed. It is found that all these design guides are compatible and agree with the extended Shields incipient motion diagram for large sediment sizes.

Several riprap design guides have been presented by various agencies [State of California (1), U.S. Army Engineering Coastal Research Center (2), U.S. Department of Transportation (3-5), U.S. Bureau of Reclamation (6,7)]. The main purpose of this study is to compare these design guides with an extended Shields diagram based on recent Chinese data for large sediment particles.

EXTENDED SHIELDS DIAGRAM FOR LARGE SEDIMENT SIZES

Riprap is used to protect riverbanks and shorelines, and the riprap size should be selected so that it cannot be moved by flows and waves. The Shields diagram (8), shown in Figure 1, has been generally recognized as a valid indication of the incipient motion of sediment particles. In this figure, K* is defined as the ratio between the forces acting on the particles and the resistance force of the particles to be moved:

$$K^* = \tau_c/(\gamma_s - \gamma_f)d \tag{1}$$

where τ_c is the time average shear stress, γ_s and γ_f are the specific weights for the sediments and fluid, respectively, and d is the diameter of the dominant sediment size.

Re_* in Figure 1 is the Reynolds number based on sediment particle sizes. This number is expressed as

$$Re_* = u_* d/\nu \tag{2}$$

where u_* is the shear velocity, d is the diameter of the sediment particle size, and ν is the kinematic viscosity of the fluid. The Reynolds number Re_* can also be treated as the ratio between the diameter of the sediment and the viscous sublayer.

If the riprap is selected so that it cannot be moved by the designed flows and waves, the riprap size should be large enough so that K* is below the Shields curve. The Shields diagram was developed for unidirectional flows only. If one uses the orbital wave velocity as the unidirectional flow velocity, the incipient motion of sediment particles under wave actions can be compared with the Shields diagram. Data and analysis for incipient sediment motion under wave action by Hou (9), Madsen and Grant (10), Bagnold (11), Komar and Miller (12), and Manohar (13) are shown on Figure 1. The averages of all the data points for wave motion seem to agree with the incipient motion curve by Shields for

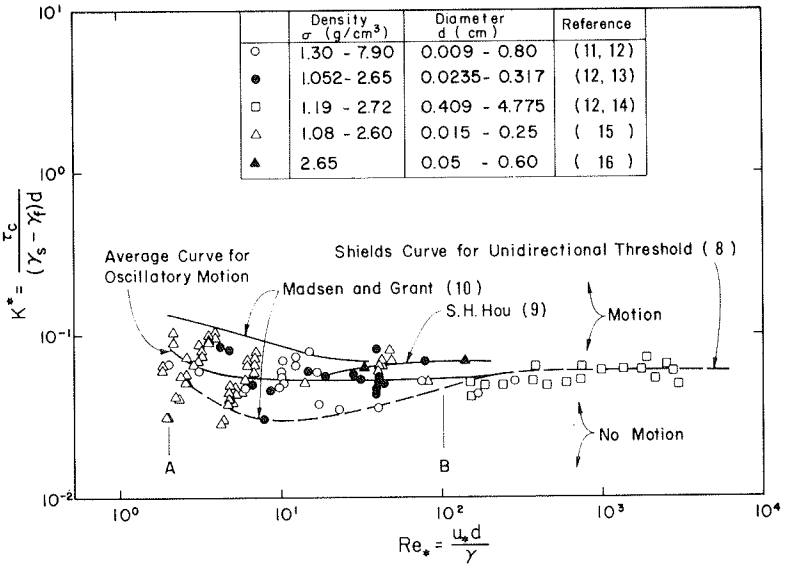

FIGURE 1 Comparison of incipient sediment motion under wave action.

unidirectional flows. The incipient motion for sediment particles under an impinged jet for high turbulent flows by Poreh and Hefez (14) was also plotted on this figure.

To use the Shields diagram to analyze various riprap guides, one must extend the diagram to large sediment sizes because the Re_* numbers for riprap are in the range of 10^4 to 10^7. For large sediment particles (Reynolds numbers 10^4 to 10^5), the drag coefficient decreases sharply. As stated by Schlichting (17):

> The influence of roughness on form drag can be summarized as follows: bodies with sharp edges, such as e.g. a flat plate at right angles to the stream, are quite insensitive to surface roughness, because the point of transition is determined by the edges. On the other hand, the drag of bluff bodies, such as circular cylinders, is very sensitive to roughness. The value of the critical Reynolds number for which the drag shows a sudden drop depends to a marked degree on the roughness . . . (p. 664).

According to this statement, the shape of the riprap should influence the drag coefficient of the sediment particles because the sediment particle shape changes the roughness of the sediment bed.

If the drag coefficient of sediment particles decreases, the drag force acting on the particle by flow will decrease and greater flows will be required to move the sediment particles. Thus the incipient motion curve of sediment particles should be moved upward (critical K* value for incipient motion should increase).

It is difficult to predict the increase in K* associated with an increase in the Reynolds number because the lift and drag forces on a sediment particle are strongly influenced by the orientation and composition of surrounding sediment particles and the intensity of the turbulence.

In China several experiments were conducted in flood channels to investigate the incipient motion of large sediment sizes. Tables 1 and 2 give data collected in Hopei and Chekiang Provinces (18). The limited data shown in Figure 2 indicate that K* increases approximately fourfold from 0.062 to 0.25 as Re_* increases from 10^4 to 10^6. This amount of increase in K* is in the same range as is the decrease in C_D, as shown in Schlichting (17). No data are available to define the dashed line for Re_* between 10^4 and 5×10^5. One may conclude from the Chinese experiments that

$$\text{For } 100 < Re_* < 1 \times 10^5 \quad \tau_c = 0.062(\gamma_s - \gamma_f)d \tag{3}$$

TABLE 1 Incipient Motion of Large Particles According to Wang (19)

Run No.	Data Source	Flow Depth (cm)	Energy Slope	Shear Stress (gm/cm^2)	Specific Particle Weight (gm/cm^3)	Median Particle Size (cm)	K*	Reynolds No.
1	Ku-Long mountain reservoir	108.0	0.014	1.51	2.65	10.7	0.086	0.412
2	Ku-Long mountain reservoir	108.0	0.011	1.19	2.65	10.7	0.067	0.397
3	Bu-Cheng River	95.0	0.009	0.855	2.65	9.65	0.054	0.280
4	Bu-Cheng River	95.0	0.0108	1.03	2.65	9.65	0.065	0.306
5	Bu-Cheng River	95.0	0.0104	0.988	2.65	9.65	0.062	0.300
6	Bu-Cheng River	80.0	0.0102	0.816	2.65	7.37	0.067	0.209
7	Bu-Cheng River	80.0	0.0081	0.648	2.65	7.37	0.0533	0.186
8	Bu-Cheng River	80.0	0.0094	0.752	2.65	7.37	0.062	0.200

TABLE 2 Incipient Motion of Large Particles According to Li (18)

Run No.	Flow Depth (cm)	Energy Slope	Shear Stress (gm/cm^2)	Specific Particle Weight (gm/cm^3)	Median Particle Size (cm)	K*	Reynolds No.
1	370.	0.06	22.2	2.70	40.0	0.326	5.90
2	330.	0.05	16.5	2.70	40.0	0.243	5.09
3	350.	0.05	17.5	2.70	40.0	0.257	5.24
4	300.	0.04	12.0	2.70	40.0	0.176	4.34
5	290.	0.04	11.6	2.70	40.0	0.171	4.27
6	260.	0.04	10.4	2.70	40.0	0.153	4.04

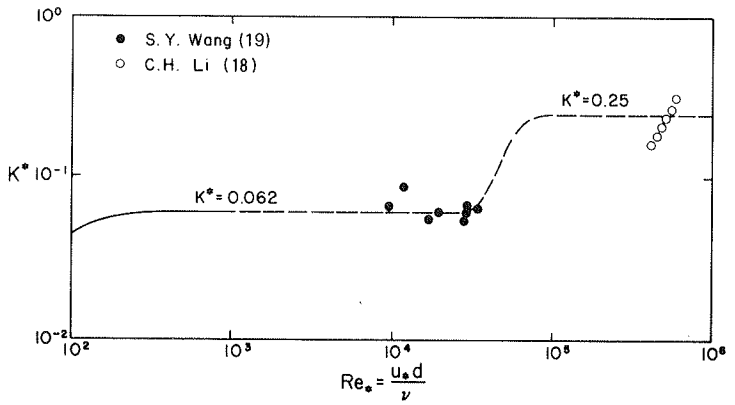

FIGURE 2 Incipient motion of large sediment particles.

and

$$\text{For } Re_* \sim 10^5 \text{ (or perhaps} > 10^5), \tau_c = 0.25\,(\gamma_s - \gamma_f)d \quad (4)$$

INCIPIENT MOTION AND RIPRAP DESIGN

Channel Revetments Under Unidirectional Flow

In the design of channel revetments, the armor stone along the channel slope should be able to withstand anticipated current velocity. The equivalent minimum size of stone diameter, d, may be calculated by the following equation that is based on an equation by the U.S. Army Coastal Engineering Research Center (CERC) (2).

$$v/(2gd)^{1/2} = y\,[(\gamma_s - \gamma_f)/\gamma_f]^{1/2}\,(\cos\theta - \sin\theta)^{1/2} \quad (5)$$

where

v = velocity of water acting directly on stone, expressed as

$$v = 5.75\,u_*\,[\log 12.27\,(h/d)] \quad (6)$$

h = flow depth;
θ = angle of structure slope with the horizontal in the direction of flow; and
y = Isbash constant, 1.20 and 0.86 for embedded and nonembedded stone, respectively.

Combining Equations 5 and 6 for y = 0.86 (nonembedded stone) and for θ = 0°, one obtains

$$K^* = 0.0447/[\log 12.27\,(h/d)]^2 \quad (7)$$

The result for a nonembedded stone condition calculated by Equation 7 is shown in Figure 3 by the solid curves.

The equivalent median stone diameter sizes are given by the U.S. Department of Transportation (U.S. DOT) in graphic form in Hydraulic Engineering Circular No. 14 (4). For a flow depth of between 1 and 3 meters, these U.S. DOT-recommended stone sizes are plotted in Figure 3. For comparison, the U.S. DOT-recommended stone sizes based on Hydraulic Engineering Circular (HEC) No. 11 (3), No. 14 (4), and No. 15 (5) are plotted together in Figure 4. The

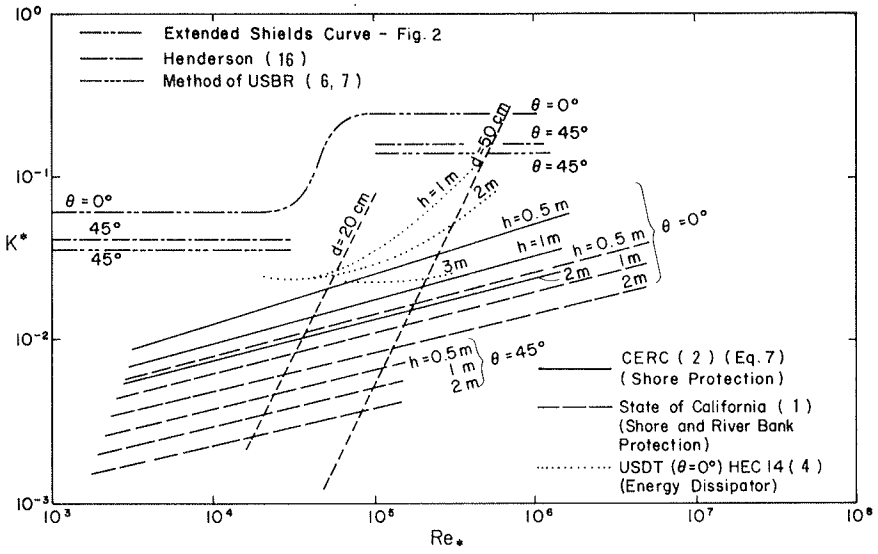

FIGURE 3 Comparison of Shields curve and data for engineering design revetments.

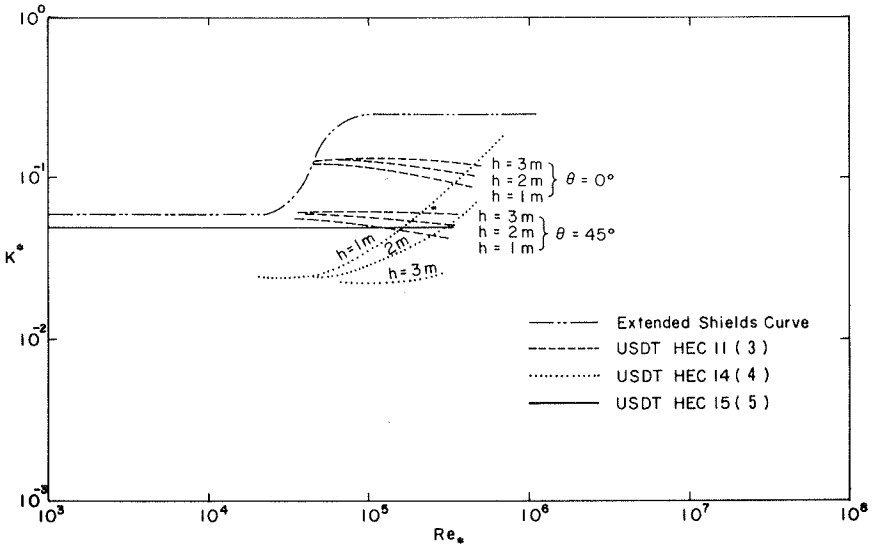

FIGURE 4 Comparison of Shields curve and U.S. DOT data.

curves for HEC No. 11 were obtained by assuming that (a) the hydraulic radius is approximately equal to the flow depth and (b) the Manning n value varies with mean stone size [i.e., $n = 0.0395\ d^{1/6}$ (5)]. Note that if the Manning n value is calculated from Strickler's formula (i.e., $n = 0.0342\ d^{1/6}$) the K* values will be lower.

The California Department of Transportation (Caltrans) presented a formula for the calculation of minimum stone sizes. The Caltrans equation may be reduced to

$$\tau_c = \left\{0.0279/[\log 12.27\,(h/d)]^2\ [\csc(\Phi - \theta)]\right\}(\gamma_s - \gamma_f)d$$
$$= \left\{0.0262/[\log 12.27\,(h/d)]^2\right\}(\gamma_s - \gamma_f)d \qquad (8)$$

where $\Phi = 70$ degrees for randomly placed rubble.

Results from Equation 8 for two different θ values ($\theta = 0$ and $\theta = 45$ degrees) and three different flow depths (h = 0.5 m, 1 m, and 2 m) are plotted as dashed curves in Figure 3.

Riprap sizes of 20 cm and 50 cm are shown as two straight lines in Figure 3. These lines are plotted on the Shields diagram and are independent of any of the riprap size recommendation curves. With a given flow condition, such as u_*, and a flow depth, the minimum riprap size can be selected as the intersection of the flow depth and riprap size for each set of recommendation curves.

For the same flow condition, the differences among the sizes recommended by the three agencies are significant. The U.S. DOT recommends the smallest riprap size. The U.S. Bureau of Reclamation (6,7) and Henderson (16) have suggested the curves shown in Figure 3 for incipient motion at the channel bed ($\theta = 0$ degree) and for incipient motion at the channel banks ($\theta = 45$ degrees).

Rubble Structures in Coastal Engineering

The following equations used to determine the stability of armor units on rubble structures in engineering may be obtained from Hou (9) and CERC (2).

$$d^* = \Phi_* H \qquad (9)$$

where

$$\Phi_* = 0.164\ \csc(\Phi - \theta')/[(\gamma_s - \gamma_f)/\gamma_f] \quad \text{(Caltrans)} \qquad (10)$$

or

$$\Phi_* = 1.24/[(\gamma_s - \gamma_f)/\gamma_f]\ K_D^{1/3}\ \cot^{1/3}\theta' \qquad (11)$$

Here

- d^* = equivalent minimum value of stone diameter,
- H = design wave height at the structure site,
- K_D = stability coefficient (2),
- θ' = angle of structure slope measured from horizontal in degrees, and
- Φ = repose angle of armor units under water surface.

According to wave theory and Equation 9, for the conditions $\gamma_S/\gamma_f = 2.65$; $\Phi = 70$ degrees; and $\theta' = 0$ degree, as derived from Equations 9 and 10, one has the result shown in Figure 5:

$$d^* = 0.106H \qquad (12)$$

From the foregoing analysis it appears that Equation 9 is not completely satisfactory because of the absence of the wave period, T, and wave number, $2\pi H/L$.

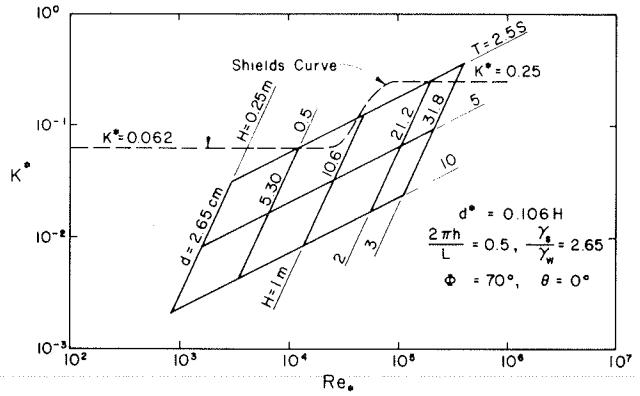

FIGURE 5 Comparison of Shields curve and data for design of rubble structure in coastal engineering.

SUMMARY AND CONCLUSIONS

The Shields diagram for incipient sediment motion has been extended for large particle size and wave environment. An extended Shields diagram is summarized in Figure 6. For Re_* numbers less than 2.0 (point A), the sediment particles are considered to be small. When Re_* numbers are greater than 100 (at point B), the K* value for incipient motion is constant. For Re_* greater than about 4×10^4, the K* value would increase 0.25 because of the decrease of drag coefficient at high Reynolds numbers. This limiting value is indicated as point C in Figure 6. However, the data are rather limited. More data are needed to establish the validity of this increase in K* value.

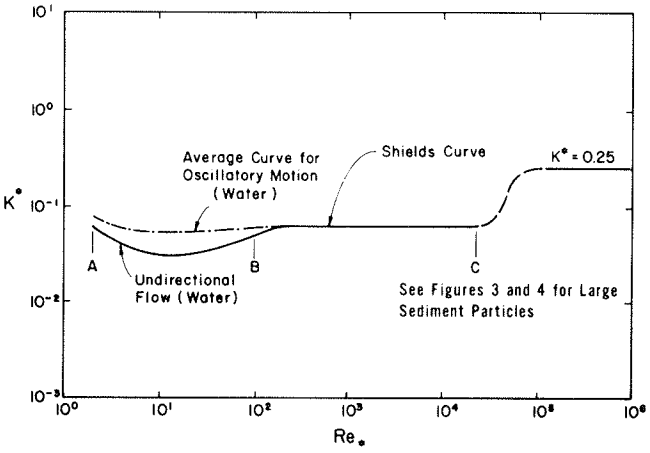

FIGURE 6 Extended Shields diagram.

For wave motion, greater flow shear stress is required to cause incipient motion; this is because of the shorter contact time between maximum orbital velocity and the sediment particle.

Riprap sizes recommended by three government agencies are plotted on the incipient motion diagram. All three agencies recommended minimum particle sizes for the design of riprap. These sizes are all below the criteria indicated by the incipient motion curves. Thus, according to incipient motion criteria, all the recommended sizes should be stable and not be moved by the flow. Caltrans seems to recommend the largest sizes and thus provides the most conservative design. All of the U.S. DOT- and

Caltrans-recommended sizes are smaller than those indicated by the incipient motion criteria. However, one must remember that actual riprap may be subjected to large turbulent fluctuation and thus much larger riprap is needed for shore protection than is indicated by the extended Shields diagram for incipient motion. Some of the riprap will protrude farther into the flow than that tested on a sediment bed under laboratory conditions. This protrusion will also affect the incipient motion of riprap.

The riprap sizes recommended by the U.S. Army Corps of Engineers and Caltrans for a wave environment are also compared with the extended Shields diagram. These recommended sizes are greater than those indicated by the incipient motion diagram. However, in addition to other factors the recommended sizes should also be a function of wave period and wave number. Recommendations for riprap sizes from various agencies are compared and analyzed according to the incipient motion diagram for different ranges of flow conditions. All the recommended riprap sizes are in the nonmotion region according to the extended Shields diagram.

Although the recommended riprap sizes are much greater than those required for incipient motion, it is not safe to use a smaller size without further study of turbulence levels near the riprap in the field and of the effect of particle protrusion into the flow. A comprehensive laboratory test should be conducted to verify the results of this study. A unified riprap design guide can then be developed.

ACKNOWLEDGMENT

The U.S. National Science Foundation sponsored this research under Grant ENG-7825056. We also wish to thank the reviewers for their comments and suggestions.

REFERENCES

1. Bank and Shore Protection in California Highway Practice. Business and Transportation Agency, California Department of Public Works, Division of Highways, 1970, pp. 101-110.
2. Shore Protection Manual, Vol. II. U.S. Army Coastal Engineering Research Center, Washington, D.C., 1973.
3. Use of Riprap for Bank Protection. Hydraulic Engineering Circular No. 11. FHWA, U.S. Department of Transportation, 1967.
4. Hydraulic Design of Energy Dissipators for Culverts and Channels. Hydraulic Engineering Circular No. 14. FHWA, U.S. Department of Transportation, 1975.
5. Design of Stable Channels with Flexible Linings. Hydraulic Engineering Circular No. 15. FHWA, U.S. Department of Transportation, 1975.
6. A.C. Carter. Critical Tractive Forces on Channel Side Slopes. Hydraulic Laboratory Report Hyd-336. U.S. Bureau of Reclamation, Denver, Colo., Feb. 1953.
7. E.W. Lane. Progress Report on Results of Studies on Design of Stable Channels. Hydraulic Laboratory Report Hyd-352. U.S. Bureau of Reclamation, June 1952.
8. A. Shields. Anwendung der Aehnlichkeits-Mechanik und der Turbulenzforschung auf die Geschiebebewegung. Preussische Versuchsanstalt fur Wasserbau und Schiffbau, Berlin, Germany, 1936.
9. S.H. Hou. Study of the Threshold of Sand Movement due to Wave Action. Science Development, Vol. 9, No. 8, 1981, pp. 645-659 (in Chinese).
10. O.S. Madsen and W.D. Grant. Quantitative Description of Sediment Transport by Waves. Proc., 15th Coastal Engineering Conference, ASCE, Vol. 102, No. CE15, July 1976, pp. 1093-1112.
11. R.A. Bagnold. Motion of Waves in Shallow Waters: Interaction Between Wave and Sand Bottom. Proc., Royal Society, London, England, Series A, Vol. 187, 1946, pp. 1-15.
12. P.D. Komar and M.C. Miller. Sediment Threshold Under Oscillatory Waves. Proc., 14th Conference on Coastal Engineering, ASCE, pp. 236-775.
13. M. Manohar. Mechanics of Bottom Sediment Movement due to Wave Action. Technical Memorandum No. 75. Beach Erosion Board, U.S. Army Corps of Engineers, 1955.
14. M. Poreh and E. Hefez. Initial Scour and Sediment Motion due to an Impinging Submerged Jet. Proc., International Association for Hydraulic Research, 1967.
15. J.C. Goddet. L'Etude du début d'entrainement des matériaux mobiles sous l'action de la houle. La Houille Blanche, No. 2, 1960, pp. 126-127.
16. F.M. Henderson. Open Channel Flow. Macmillan, New York, 1966.
17. H. Schlichting. Boundary-Layer Theory, 7th ed. McGraw-Hill, New York, 1979.
18. C.H. Li. The Criteria of Threshold Shearing Stress and Ripple Formation: Experimental Results in Glycerine Flow. Report No. 70. Nanjin Hydraulic Research Institute, Republic of China, 1965 (in Chinese).
19. S.Y. Wang. Stability of Alluvial Rivers. Tianjin University Technical Report. Republic of China, 1975 (in Chinese).

Publication of this paper sponsored by Committee on Hydrology, Hydraulics and Water Quality.